analytical chemistry

Article

pubs.acs.org/ac

Exploring the Interactome: Microfluidic Isolation of Proteins and Interacting Partners for Quantitative Analysis by Electron Microscopy

Dominic Giss, Simon Kemmerling, Venkata Dandey, Henning Stahlberg, and Thomas Braun*

Center for Cellular Imaging and Nano Analytics, Biozentrum, University of Basel, Basel 4056, Switzerland

Supporting Information

ABSTRACT: Multimolecular protein complexes are important for many cellular processes. However, the stochastic nature of the cellular interactome makes the experimental detection of complex protein assemblies difficult and quantitative analysis at the single molecule level essential. Here, we present a fast and simple microfluidic method for (i) the quantitative isolation of endogenous levels of untagged protein complexes from minute volumes of cell lysates under close to physiological conditions and (ii) the labeling of specific components constituting these complexes. The method presented uses specific antibodies that are conjugated via a photocleavable linker to magnetic beads that are trapped in microcapillaries to immobilize the target proteins. Proteins are released by photocleavage, eluted, and subsequently analyzed by quantitative transmission electron microscopy at the single molecule level. Additionally, before photocleavage, immunogold can be employed to label proteins that interact with the primary target protein. Thus, the presented method provides a new way to study the interactome and, in combination with single molecule transmission electron microscopy, to structurally characterize the large, dynamic, heterogeneous multimolecular protein complexes formed.

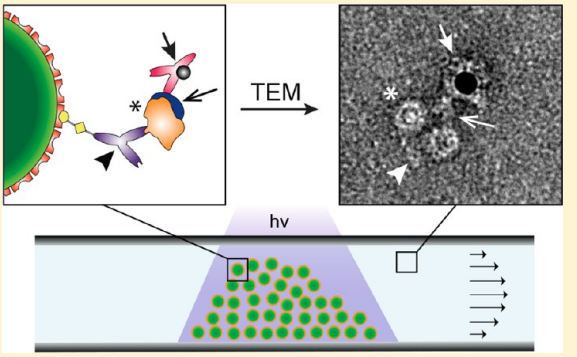

Systems biology aims to identify and quantify the molecular elements of biological systems, to determine the dynamic interactions between them, and to integrate the resulting information into system networks.[1] The development of these holistic models necessitates the quantitative detection of protein-interaction assemblies and their characterization in terms of stoichiometry, structure, and temporal persistence. The stochastic nature of biological processes makes the analysis of these heterogeneous, multimolecular complexes at the single molecule level essential.

Many experimental strategies are used today to characterize the proteome of cells[2,3] or to define the interactome.[4,5] In these, protein complexes are often identified using hybrid approaches relying on affinity purification or immunoprecipitation in combination with chemical cross-linking[6] or gel electrophoresis[7] and mass spectrometry.[8] These methods analyze a sample from multiple cells and quantify the average relative occurrence and composition of the available protein complexes. Due to the large number of protein copies required, these methods are generally not well suited for the analysis of heterogeneous, multimolecular protein complexes, such as the human Mediator complex,[9] transiently formed during interaction pathways. Further, although proteins interacting within a complex can be defined,[10] the structure of the entire multimolecular complex remains unknown. However, the structure of the entire complex has to be known to fully understand the role of the complex in the cell.

Electron microscopy can be used to image single molecules and obtain various types of structural information.[11,12] For example, cryo-electron tomography (cryo-ET) can provide information at molecular resolution for larger proteins in unperturbed single cells.[13−15] However, *visual proteomics* by electron tomography[16] is restricted to small cells or to sections of cells (the sample diameter must be below 1 μm for cryo-ET to reach higher resolution),[17] and protein recognition is limited to relatively large protein complexes.[18,19] Further, the identification of complexes and their constituents without electron dense labels[20] in intact cells is challenging. We have recently developed a new approach to visual proteomics in which eukaryotic cells are lysed and the proteins in the lysate and membrane fragments are visually analyzed by single molecule transmission electron microscopy (TEM).[21,22] Again, without the aid of electron dense labels, interpretation can be ambiguous. However, in this case, the cell lysate is easily accessible for labeling methods.

Here, we present a fast microfluidic protein isolation method and demonstrate its use with TEM for the extraction of protein assemblies from cell lysate and their quantification. The method allows endogenous levels of untagged protein complexes to be specifically isolated from minute volumes of complex biological background and investigated at the single molecule level. It provides initial structural information. Importantly, the approach also allows interacting partners to be identified by a

Received: September 2, 2013
Accepted: April 11, 2014

 © XXXX American Chemical Society dx.doi.org/10.1021/ac4027803 | *Anal. Chem.* XXXX, XXX, XXX−XXX

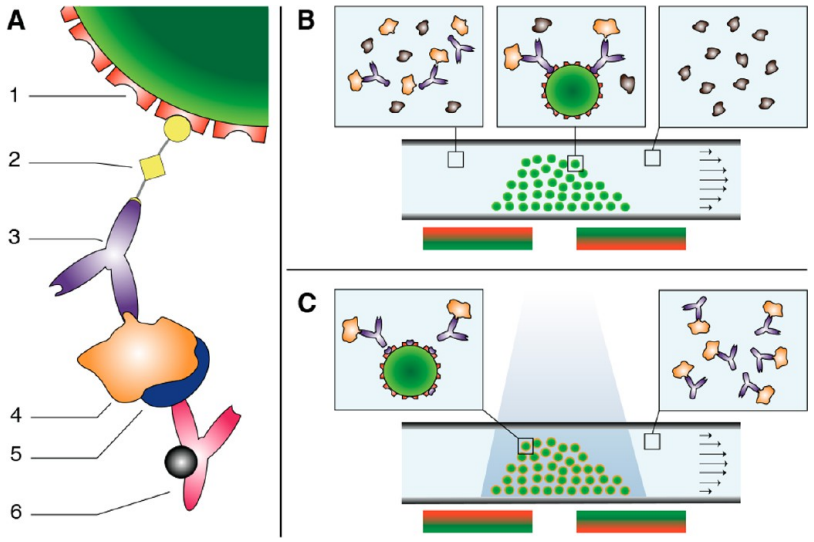

Figure 1. Principle of the microfluidic affinity isolation method. (A) AB-biotin conjugates bound to a streptavidin-coated magnetic bead. 1: Streptavidin-coated magnetic bead of 1 μm in diameter; 2: photocleavable NHS-biotin cross-linker; 3: AB against the target protein; 4: target protein; 5: protein binding partner (optional); 6: immuno-gold labeled AB against the binding partner. (B) Affinity extraction. Streptavidin-coated magnetic beads are trapped in a microcapillary (inner diameter of 250 μm) using two external magnets positioned underneath the capillary. After loading, the capillary is rinsed with sample solution that was previously incubated with biotinylated ABs against the target structure. The capillary and beads are then washed to remove other proteins; ABs and their targets remain immobilized. Optionally, the capillary can next be rinsed with potential binding partners of the target structures and/or with immuno-gold ABs to label immobilized target proteins or their interacting partners. (C) Photocleavage and elution. Target structures are recovered by illuminating the beads with UV-light at a wavelength of 365 nm and eluting the released AB-target protein complexes. Downstream applications such as TEM analysis follow.

labeling step, here termed interaction labeling, and the intact complex to be visualized by TEM.

■ EXPERIMENTAL SECTION

Working Principle. The approach is based on antibodies (ABs) that are conjugated to a photocleavable biotin cross-linker[23] (Figure 1A). These conjugates interact with streptavidin-coated magnetic beads that are immobilized in microcapillaries by a magnetic trap (Figure 1B; Supporting Information Figure S1). The basic protocol is as follows: Cell lysate is mixed with biotinylated ABs against the target protein and passed over the trapped beads. Subsequently, the capillary is rinsed with buffer to wash out all unbound proteins. Finally, the immobilized target proteins are released by illuminating the capillary with UV-light at a wavelength of 365 nm to photocleave the cross-linker. Target proteins are then eluted and loaded on TEM grids (Figure 1C). This protocol can be extended by two variations before photocleavage and elution: (i) A labeling step using immunogold can be included to identify and localize the target proteins or their copurified interacting partners in a protein assembly; (ii) extracted proteins can be used as bait to "fish" for potential binding partners, again followed by a labeling step.

Separation Setup. A 250 μm inner-diameter fused silica capillary (BGB Analitik AG #TSP-250350, Switzerland) was guided through a lens tube construction cube (Thorlabs #SM1C6, Germany) so that optical components could be easily mounted and to provide protection from UV-light (Supporting Information Figure S1). The outer polymer coating of the capillary was thermally removed from a 1 cm-long length region at the center of the cube to avoid absorbance of UV-light. Magnetic beads were trapped in the stripped region by two external permanent magnets (Supermagnete #Q-20-10-05-N, Switzerland) positioned below the capillary at the center of the cube. UV-light at 365 nm was emitted by a high power UV LED (Thorlabs #M365L2, Germany) mounted on top of the cube and guided onto the magnetic beads using collimator and focusing lenses (Thorlabs #LA1952 and #LA1131, Germany). Liquids were aspirated or dispensed via a stepper motor syringe pump (Genie Pump, Kent Scientific) from 200 μL PCR tubes mounted on an *xy*-stage.

Loading of Magnetic Beads. About 40×10^6 streptavidin-coated magnetic beads with a diameter of 1 μm (corresponding to 4 μL of the beads employed; Dynabeads MyOne, Invitrogen #656-01, Switzerland) presented in phosphate buffered saline (PBS) were aspirated into a 250 μm inner-diameter fused silica capillary at a flow rate of 20 μL/min. An external permanent magnet positioned in close proximity below the capillary caused a plug of beads to form (Supporting Information Figure S1). After this bead-loading step, a second magnet was added to fully trap the plug, and the beads were rinsed with the buffer used for the subsequent experiment. In this manner, a robust, 3−4 mm long plug was formed and equilibrated with the required buffer.

Antibody Biotinylation. ABs were incubated with a 10-fold molar excess of photocleavable NHS-biotin cross-linker (Ambergen, USA) for 1.5 h at pH 8.2. After incubation, the mixture was dialyzed overnight against 2 l of PBS (phosphate buffered saline, 0.01 M phosphate buffer, 0.0027 M potassium chloride, and 0.137 M sodium chloride, pH 7.4, Sigma-Aldrich #P4417, Switzerland) using dialysis buttons (membranes with a 13 kDa cutoff) to remove unbound cross-linker.

Extraction and Purification of Target Structures. A stock solution of apoferritin (AF) from equine spleen in 50% glycerol (Sigma-Aldrich #A3660, Switzerland) was diluted to 3−300 nM using baby hamster kidney (BHK) cell lysate. The AF/cell lysate mixtures were incubated for 1 h on ice with biotinylated polyclonal antihorse spleen ferritin ABs produced in rabbit (Sigma-Aldrich #F6136, Switzerland; henceforth

dx.doi.org/10.1021/ac4027803 | *Anal. Chem.* XXXX, XXX, XXX−XXX

termed antiferritin ABs) at 47 nM concentration. Subsequently, 2 μL of the mixture was passed over trapped magnetic beads for 15 min to immobilize target proteins on the beads. The actual incubation time of the biotinylated ABs with the streptavidin-coated beads was about 60 s on average. Finally, the capillary was rinsed with PBS to remove unbound proteins. Progress of the washing process was probed by collecting a series of eluted wash fractions and analyzing them by TEM.

To demonstrate that immobilized proteins can be used as bait for potential binding partners, 2 μL of a 1 nM solution of polyclonal antihorse ferritin antibodies produced in goat (Lubio Science #A70-128A, Switzerland) was diluted with BHK cell lysate and passed over previously immobilized AF for 15 min. After incubation, the capillary was rinsed with PBS to completely separate trapped ABs from cell lysate. Immobilized goat antiferritin ABs were then labeled with 10 nm of colloidal immunogold by rinsing the capillary with 2 μL of antigoat IgG gold (Sigma-Aldrich #G5402, Switzerland) diluted 1:10 in 0.1% BSA (Sigma-Aldrich #A3294, Switzerland) for 15 min.

To extract endogenous 26S proteasome, HEK293 cell lysate was incubated with biotinylated polyclonal anti-20S proteasome ABs from rabbit (Merck Millipore #ST1053) for 120 min on ice. Four μL of the mixture, corresponding to the lysate of about 40 thousand cells, was then passed over immobilized magnetic beads during a time period of 15 min. Washing steps were carried out with HEPES buffer (25 mM HEPES-KOH, pH 7.4; 5 mM $MgCl_2$ and 10% glycerol).

The isolation of endogenous TCP-1 ring complex (TRiC) from HEK293 cell lysate was performed using biotinylated monoclonal anti-CCT epsilon ABs (Pierce Antibodies #MA1-82643) and HEPES buffer (20 mM HEPES-KOH, pH 7.4; 5 mM $MgCl_2$; 50 mM NaCl and 10% glycerol).

Recovery of Target Structures. Immobilized target proteins were released from the magnetic beads by illuminating the plug in the capillary with UV-light for 10 min to cleave photocleavable biotin. Photocleavable biotin shows maximal absorbance around 270 nm but still has distinct absorbance at 365 nm, the wavelength emitted by the UV LED employed. After cleavage, analytes were eluted in 3−6 μL of buffer and collected.

Washing Procedure. After each incubation step, the capillary was rinsed with buffer (PBS or HEPES buffer, depending on the experiment) to separate unbound from immobilized proteins. Depending on the applied cell lysate concentration, the immobilized beads were washed for 5−25 min at 20−40 μL/min flow rates. After an experiment, the magnetic beads were discarded by pressurizing the capillary. The latter was then extensively washed with double-distilled H_20, 70% EtOH, and 0.1 M NaOH.

Cell Preparation. Adherent baby hamster kidney fibroblasts (BHK21; ECACC 85011433) and 293 cell line human embryonic kidney cells (HEK293; ECACC 85120602) were cultured in polystyrene T75-flasks containing 30 mL of DHI-5 medium (see below) for BHK cells and 10 mL of culture medium (see below) for HEK293 cells, at 37 °C and 5% carbon dioxide. To split the cells, the medium was removed and the flask was washed with 10 mL of 37 °C warm PBS w/o calcium and magnesium (Dulbecco's phosphate buffered saline, Sigma-Aldrich #D8537, Switzerland). To detach the cells, 3 mL of trypsin-EDTA solution (0.05% trypsin 0.53 mM EDTA, Invitrogen #25300-054, Switzerland) was added and drained before the cells were incubated at 37 °C for 5 min. The detached cells were diluted with 10 mL of 37 °C warm medium and homogenized using a pipet. For BHK cells, 0.5 mL of the homogenized cell suspension and 30 mL of fresh medium were returned to the flask for further cultivation. For HEK293 cells, 1 mL of the homogenized cell suspension and 9 mL of fresh medium were used. The rest of the cell suspension was washed twice with PBS and concentrated to a final cell concentration of 1000 cells/μL for BHK cells or 10 000 cells/μL for HEK cells using PBS or HEPES buffer (depending on the experiment). In both cases, cells in 0.5 mL of the suspension were then physically lysed by sonication for 30−60 s using a tip sonicator while cooling. The fresh lysates were either directly used for experiments or aliquoted and stored at −80 °C.

DHI-5 medium is a 1:1:2 mixture of DME (Dulbecco's modified Eagles medium, Sigma-Aldrich #D6171, Switzerland), HamF12 (Nutrient mixture F-12Ham, Sigma-Aldrich #N8641, Switzerland), and IMDM (Iscove's modified Dulbecco's medium, Sigma-Aldrich #I3390, Switzerland) media, supplemented with 5% FCS (Fetal calf serum, Sigma-Aldrich #E7524, Switzerland) and complemented with nonessential amino acids (MEM nonessential amino acid solution, Sigma-Aldrich #M7145, Switzerland), L-glutamine (L-glutamine solution, Sigma-Aldrich #G7513, Switzerland), and vitamins (RPMI1640 vitamins solution, Sigma-Aldrich #R7256, Switzerland). For HEK293 cells, the culture medium was EMEM (Eagle's minimal essential medium, Sigma-Aldrich #M2279, Switzerland) supplemented with 10% FCS and complemented with nonessential amino acids and L-glutamine.

TEM Grid Preparation. Immediately after elution, 3 μL of the eluted analytes was incubated for 90 s on glow-discharged carbon coated copper TEM grids (200 mesh). After a blotting step, grids were washed five times for 12 s with double-distilled H_2O and negatively stained with two 4.5 μL drops of 2% uranylacetate. After every incubation and the final washing step, excess liquid was removed using blotting paper.

Image Acquisition and Processing. Automated image acquisition was done on a FEI T12 operated at 100 kV using the Leginon 2.1 (incl. in Myami 2.1) software.[24] The images were recorded on a Gatan 2k × 2k CCD camera. A semiautomatic image acquisition routine was used for the quantitative analysis of analytes (Figure 2): First, five squares of the TEM grid were manually selected for analysis. Then, a mesh consisting of 35 subsquares was created within every square, and 11 images per subsquare were automatically acquired at 12 000× magnification (pixel size: 0.8725 nm; defocus: 0.8−1.4 μm; dose: 22−35 electrons/$Å^2$). Thereby about 12% of the area of a particular square was imaged. Subsequently, using the 1925 images collected per grid, target proteins were identified by their visual appearance in negative stain and counted. This was done manually and/or using the Appion 2.1 (incl. in Myami 2.1) software[25] in combination with a template picking routine.[26] Note that ABs often linked targets to form multiprotein complexes. In this case, every target unit was counted individually.

Manual TEM was carried out on a Philips CM10 operated at 80 kV. The images were recorded on a 2k × 2k CCD camera (Olympus SIS, Münster, Germany). For 2D class averages, images were acquired at 130 000× nominal magnification (pixel size: 0.37 nm; defocus: 0.1−0.3 μm). Particles were picked manually using EMAN2 software package,[27] classified, and averaged using the e2refine2d algorithm.

dx.doi.org/10.1021/ac4027803 | Anal. Chem. XXXX, XXX, XXX−XXX

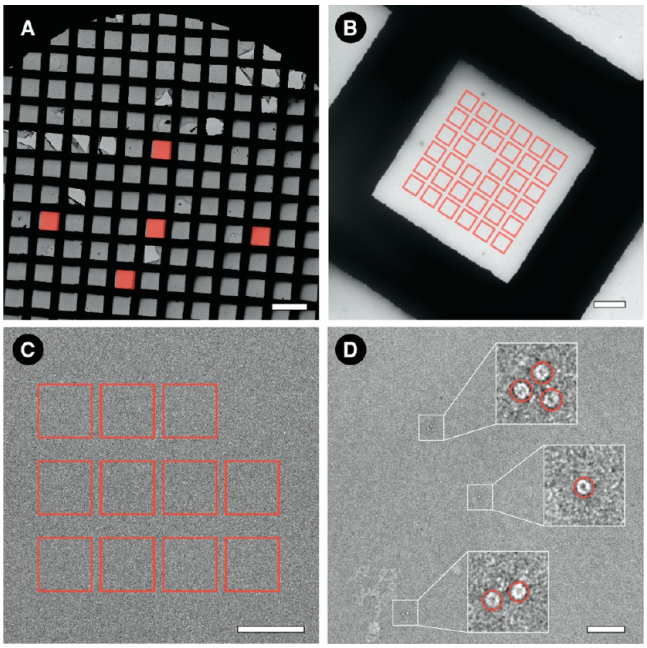

Figure 2. Semiautomatic TEM procedure for image acquisition and data-analysis. (A) Step 1: Manual selection of five squares of a TEM grid. (B) Step 2: The procedure targets 35 subsquares per grid square. (C) Step 3: 11 images are recorded per subsquare. (D) Step 4: Image processing. Particles of interest are detected by their visual appearance in negative stain on the total of 1925 images per grid either manually or automatically using a template and counted; each AF was counted as one particle, regardless of whether it was associated with other AFs or not. Scale bars, 200 μm (A), 20 μm (B), 2 μm (C), and 200 nm (D).

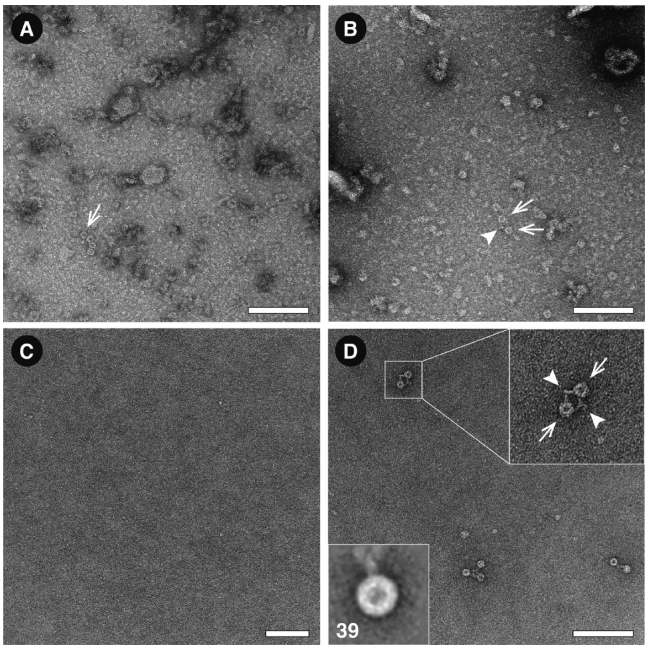

Figure 3. Affinity extraction and recovery of apoferritin. (A) The initial cell lysate/30 nM AF (arrow) mixture. The mixture was incubated with biotinylated antiferritin ABs (47 nM) and passed over streptavidin-coated magnetic beads immobilized by a magnetic trap in a microcapillary, and the capillary was subsequently washed with buffer. (B) First wash fractions document that crude cell lysate does not obstruct the capillary and that not every single AF (arrow)-AB (arrowhead) complex was extracted. (C) Last wash fraction, confirming that unbound proteins were removed by the washing process. (D) Eluate after photocleavage of the cross-linker showing recovered AF (arrow)-AB (arrowhead) complexes; these have been cleanly isolated from the cell lysate. Inset: 2D class average (bottom left, number of averaged particles) of recovered AF with visible AB attached. Scale bars, 100 nm.

RESULTS AND DISCUSSION

We have developed a quantitative method that enables the fast and specific extraction and recovery of target proteins from minute volumes of cell lysate without the need for genetic engineering to introduce affinity tags. Samples are deposited on TEM grids and examined at the single molecule level by quantitative TEM (qTEM), which also delivers structural information by single particle analysis. Our method also allows potential binding partners to be detected and analyzed. These interaction partners either copurify with the primary target protein or can be "fished" from complex samples using a previously isolated protein as bait. Immunogold labeling both aids protein identification and localizes specific proteins in the extracted multimolecular complexes.

To quantitatively assess the method, we complemented the crude cell lysate obtained from sonicated BHK cells with known amounts of AF as target protein and incubated this lysate with biotinylated antiferritin ABs. Two μL of the mixture (total amount of AF, 6−600 fmol, depending on the experiment) was passed over previously immobilized magnetic beads during a time period of 15 min, followed by 200 μL of PBS during a time period of 10 min. Photolysis was carried out for 10 min after this washing step, and the released AF-AB complexes were eluted in 6 μL of PBS for TEM analysis. The excess of streptavidin-coated magnetic beads offered ample binding surface for the biotinylated ABs; as expected, control experiments showed that using more beads did not improve extraction efficiencies.

An example of the isolation process is shown in Figure 3. The first wash fractions after the immobilization step contained BHK cell lysate and some nonextracted AF (Figure 3B), recognizable by its typical ring-shaped projection (compare Supporting Information Figure S2). Most of the unbound proteins were removed by the washing procedure (Figure 3C). AF-AB complexes were recovered after the subsequent photocleavage step (Figure 3D). The clean background in this image documents the very low concentration of contaminants on the TEM grids. Proteins that were non-specifically bound to the beads were not released by the photocleavage step (compare Figure 3D and Supporting Information Figure S3).

We performed qTEM to analyze the results of the isolation experiments. A semiautomatic, TEM image acquisition and data analysis procedure was developed for this (Figure 2). Thereby, 1925 images were recorded from defined regions of each TEM grid and the target proteins were detected by their visual appearance and counted, allowing the total amount of recovered protein to be measured. Running a series of experiments as described above, with concentrations of the target protein AF ranging from 3 to 300 nM and an AB concentration of 47 nM, yielded the signal transfer function (SiTF, Figure 4 and Supporting Information Figure S4) of the method for AF. This quantitative measurement reflects the AB-antigen binding curve (Figure 4). Using the Hill equation for noncooperative binding to extract the *apparent* dissociation constant K_d of the AB-AF interaction from the recorded data

dx.doi.org/10.1021/ac4027803 | *Anal. Chem.* XXXX, XXX, XXX−XXX

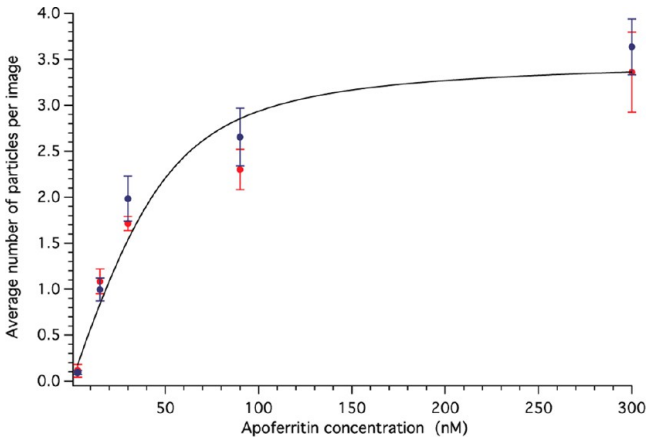

Figure 4. Signal transfer function of the microfluidic affinity isolation method for AF determined by qTEM. To quantitatively assess the response of the developed method, we processed different concentrations of AF, ranging from 3 to 300 nM, using a constant amount of antiferritin ABs (47 nM). Two TEM grids were prepared for every experiment (red and blue symbols). In a semiautomatic manner, 1925 images were collected per grid (385 per selected grid square), and AF was detected by its visual appearance in negative stain and counted (see Figure 2). The average number of AF particles per image (PPI) for the particular grid is shown. Error bars represent the standard deviation of the average PPIs of the five probed grid squares of the parent grid. The data reflects the AB-antigen binding curve for an increasing antigen concentration, which was modeled (black line) using Hill's equation.

gave an apparent K_d of 12 nM. Control experiments showed that the SiTF of AF to TEM grids depends linearly on the applied concentration of AF (Supporting Information Figure S5). These experiments show that the AB binding characteristics dominates the SiTF of the presented isolation method.

We used HEK293 cell lysate to demonstrate the extraction and recovery of endogenous levels of protein complexes from cell extract by our one-step isolation method. In these experiments, we added biotinylated anti-20S proteasome ABs to the cell lysate to bind endogenous 26S proteasomes and processed the lysate of about 40 thousand HEK293 cells suspended in HEPES buffer. The protocol was similar to that described for AF. A typical experiment, starting with the lysis of cells and ending with the isolated target protein on TEM grids, took approximately 160 min, including an AB-target protein incubation step of 2 h. As depicted in Figure 5, the method enabled us to isolate intact 26S proteasomes composed of a 20S core complex and two weakly interacting 19S regulatory units from cell extract, as well as 20S proteasomes lacking one or both of the 19S regulatory complexes. The isolation of fully assembled 26S proteasomes, which are sensitive to buffer conditions (Supporting Information Figure S6), clearly demonstrates that complexes formed by weakly interacting proteins can be isolated by the proposed method. Furthermore, using biotinylated anti-CCT ABs, we isolated endogenous levels of TRiC (Figure 5D). Note that the application of unspecific ABs (or no ABs at all) did not result in the isolation of target proteins.

The proteasomes and TRiC can be visually identified in negative stain TEM images due to their characteristic size and shape. The average structures calculated by single particle analysis are in excellent agreement with previously reported models[28−30] and 2D class averages of purified 20S proteasomes (Supporting Information Figure S7). Sometimes, ABs are visibly attached to the proteins; therefore, we can be confident that the isolated particles are indeed the target protein complexes and that the corresponding structural analysis is relevant.

Additionaly, immunogold markers can be used to unambiguously detect specific proteins and localize them within a complex. Exploiting this, we used immobilized target proteins to fish for potential binding partners and identified them by gold tags (Figure 1A). As a proof of concept, AF was mixed with BHK cell lysate and biotinylated rabbit antiferritin ABs and immobilized on magnetic beads as described above. To mimic binding partners, the capillary was subsequently flushed for 15 min with a total of 2 μL of 1 nM goat antiferritin AB solution in BHK cell lysate. After washing, the capillary was rinsed for 15 min with 2 μL of antigoat colloidal gold to label established protein complexes. Photolysis and the elution of AF-AB complexes for TEM analysis followed. As shown in Figure 6, the approach allows binding partners (arrow) to be (i) fished and recovered from complex backgrounds and (ii) identified by an attached immunogold label (arrowhead). In our studies, we did not detect any cross-reactivity between antigoat immunogold and rabbit ABs or AF.

The presented method uses functionalized magnetic beads to form bead plugs in microcapillaries by magnetic trapping. This approach significantly reduces the diffusion path length required for protein binding and offers a massive increase in the available binding surface compared to, for instance, functionalized capillary walls. The technique provides a fast and convenient way to process submicroliter volume samples. Important for future high-throughput applications, the immobilization or release of beads can be easily tuned by adjusting the applied magnetic field gradient, enabling their rapid exchange.[31]

The use of photocleavable linkers allows sample recovery under mild conditions that conserve the structural integrity of proteins. It is not necessary to use relatively harsh methods such as boiling the beads, treatment with low pH buffers, or changing the salt concentration, all of which might affect the structural integrity of target proteins or lead to disassembly of protein complexes. Indeed, the photocleavage employed is carried out at a wavelength of 365 nm, which is not significantly absorbed by most protein targets and therefore does not interfere with their structures or the complexes formed. Moreover, finite element simulations estimate that the UV-light induced temperature rise experienced by capillaries and buffers is lower than 0.6 °C (Supporting Information Figure S8). Elution by photocleavage is more specific than traditional chemical procedures and serves as a second "purification" step; proteins that are nonspecifically bound to the immobilized beads or the capillary surface are not released (Supporting Information Figure S3). This explains the low contaminant concentration in the eluates, as indicated by the almost perfectly clean background of the TEM images (Figures 3D, 5, and 6). The purity of the eluates facilitates qTEM and structural analysis of the individual complexes. Furthermore, we have demonstrated that weak interacting protein complexes, such as the regulatory 19S and the 20S core particle forming a 26S proteasome, survive the isolation procedure (Figure 5A,B).

Quantitative TEM showed that the amount of recovered target protein depends on the initial concentration of the protein in the cell extract (Figure 4). Once the respective SiTF of a target protein has been calibrated (Figure 4 and Supporting Information Figures S4 and S5), absolute quantities can be

dx.doi.org/10.1021/ac4027803 | Anal. Chem. XXXX, XXX, XXX−XXX

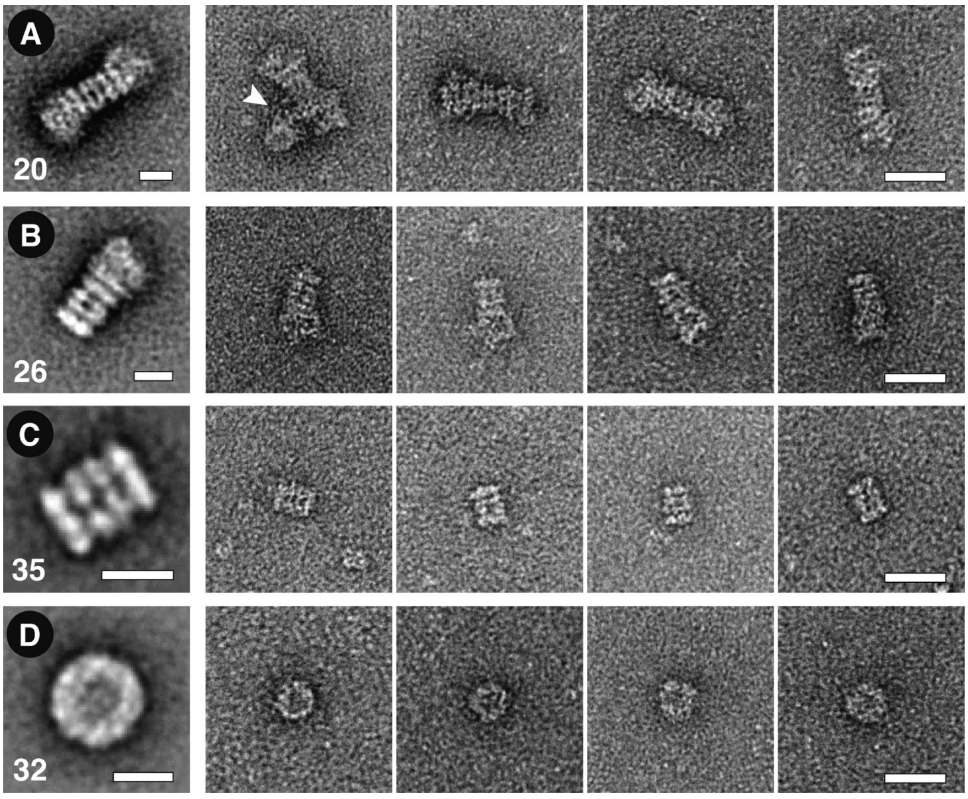

Figure 5. Isolation of endogenous protein complexes. HEK293 cell lysate was incubated with biotinylated anti-20S proteasome ABs (A, B, C) or biotinylated anti-CCT ABs, respectively (D). The lysate of about 40 thousand cells was then passed over trapped streptavidin-coated magnetic beads to extract target complexes, which were subsequently recovered by photocleavage and transferred onto TEM grids. Left panels: Representative 2D class averages of isolated target structures (bottom left, number of averaged particles). Scale bar, 10 nm. Right panels: Gallery of negatively stained particles. Scale bar, 25 nm. (A) 26S proteasomes, composed of two regulatory 19S particles and the 20S core proteasome. In rare cases, we found complexes linked by ABs (arrowhead). (B) Partially disassembled proteasomes, lacking one of the regulatory 19S particles. (C) Side view of isolated 20S core particles. (D) TRiC. Typical ring-shaped top views, 16 nm in diameter, are visible.

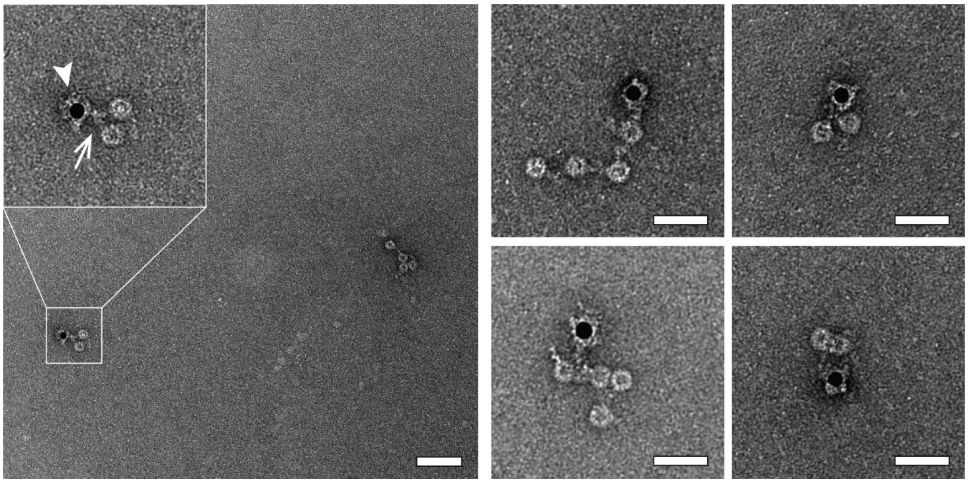

Figure 6. The detection of extracted protein binding partners by interaction labeling. AF in a mixture of cell lysate and biotinylated antiferritin ABs was immobilized on the streptavidin coated magnetic beads, where it acted as bait protein. In a second step, the capillary was then rinsed with goat antiferritin ABs (arrow) supplied in cell lysate to mimic potential binding partners. In a third step, the capillary was rinsed with antigoat colloidal gold (10 nm, arrowhead) to label the fished goat antiferritin ABs and, thus, facilitate the detection of established interactions by TEM. The complexes were recovered by photocleavage and transferred onto TEM grids. The black spots on the images are gold particles labeling the goat antiferritin ABs. Scale bars, 50 nm.

measured. To our knowledge, this is the first time where the feasibility of single molecule qTEM for protein quantification has been demonstrated. As shown in Figure 4, the SiTF of protein is dominated by the antibody-antigen binding curve, which also allows the apparent binding constant to be determined. Further, the method provides reproducible results; the resulting particle concentrations on two TEM grids prepared with the same sample differ by maximally 15%

dx.doi.org/10.1021/ac4027803 | *Anal. Chem.* XXXX, XXX, XXX–XXX

(peak-to-peak). The measurement variations of other methods used for protein quantification, e.g., reverse phase protein arrays, are comparable.[32]

As indicated in Supporting Information Figure S4, the SiTF of the presented isolation method depends on four main factors. Future improvements to their experimental aspects will result in more target proteins being isolated and detected: First, the use of smaller affinity molecules with only one binding site and higher binding constants, such as DARPins,[33] nanobodies[34,35] or aptamers[36] instead of ABs, should increase the extraction efficiency of target structures. Second, the use of techniques enabling a much more efficient transfer of proteins onto TEM grids, such as the "sample writing" procedure that we described in Kemmerling et al.,[22] will significantly increase the concentration of particles on TEM grids. Third, new camera types[37] will allow isolated particles to be imaged faster with a massively improved signal-to-noise ratio and counted more accurately. Fourth, improved algorithms for particle detection will allow the analysis of larger data sets with better precision. Together, this will make the image acquisition and/or quantitative analysis less time-consuming and improve the sensitivity and detection limits of the technique. However, already now the method presented can be applied to collect enough images of well-distributed particles to calculate class averages of the isolated target structures (Figures 3 and 5). The presence of ABs did not interfere with 2D class averaging (Supporting Information Figure S6). Class averages can aid protein identification and provide initial structural information. Further, if their signal is not averaged out (inset Figure 3D), bound ABs revealed in the average can be used to localize specific subunits in a complex.[30]

Figure 6 demonstrates the detection of extracted protein binding partners by immunogold labeling. In general, two problems must be overcome to detect binding partners by immunotagging: First, specific and efficient labeling must be achieved. Second, unbound label must be removed, or ways to discriminate between label specifically bound to the protein and label randomly adsorbed to the TEM grid must be found. The method presented provides an elegant and efficient way to remove unspecific label before elution of the protein complexes and TEM grid preparation, thus avoiding the second hurdle.

CONCLUSIONS

We have presented a fast, one-step affinity isolation method for the quantitative extraction of endogenous levels of protein from complex samples without significant contaminants. Furthermore, protein-protein interactions can be probed and interacting partners can be labeled for subsequent structural analysis at the single molecule level by qTEM. This allows the composition, conformation, and the structure of individual protein assemblies to be investigated. Moreover, quantitative conclusions can be drawn, since relative or even absolute quantification of protein levels can be achieved. This will allow the study of, e.g., pulse chase experiments inducing changes in protein complexes such as inflammasomes,[38] not only on a functional and structural but also on a quantitative level. We foresee that, in combination with novel grid preparation techniques, the use of single binding site affinity proteins, and a new class of detectors in electron microscopy, this methodology will facilitate the processing of single cell extracts by "lyse and spread" visual proteomics[21,22,39] and ultimately will offer a completely new way to study the interaction networks of protein complexes in individual cells.

ASSOCIATED CONTENT

Supporting Information

Supporting figures (Figures S1−S8) showing a photograph of the experimental setup, an electron micrograph and 2D class averages of apoferritin, an electron micrograph of nonspecifically bound proteins, a diagram indicating the factors determining the signal transfer function of the method, the signal transfer function of apoferritin to TEM grids, the isolation of endogenous 20S proteasome in PBS buffer, an electron micrograph and 2D class averages of purified 20S proteasomes, and the results of COMSOL simulations of the UV-light induced temperature rise in capillary and buffer. This material is available free of charge via the Internet at http://pubs.acs.org.

AUTHOR INFORMATION

Corresponding Author

*E-mail: Thomas.braun@unibas.ch. Phone: +41-61-387-32-28. Fax: +41-61-387-39-86.

Notes

The authors declare no competing financial interest.

ACKNOWLEDGMENTS

We thank Shirley Müller and Benjamin Bircher (C-CINA, University of Basel, Switzerland) for carefully reading the manuscript and expert discussions. The project was supported by the SNF SystemsX.ch (CINA, granted to H.S.) and the NCCR Nanoscience.

REFERENCES

(1) Aderem, A. *Cell* **2005**, *121*, 511−513.
(2) Fields, S.; Song, O. *Nature* **1989**, *340*, 245−246.
(3) Walther, T. C.; Mann, M. *J. Cell Biol.* **2010**, *190*, 491−500.
(4) Uzoma, I.; Zhu, H. *Genomics, Proteomics Bioinf.* **2013**, *11*, 18−28.
(5) Vidal, M.; Cusick, M. E.; Barabasi, A. L. *Cell* **2011**, *144*, 986−998.
(6) Klockenbusch, C.; Kast, J. *J. Biomed. Biotechnol.* **2010**, *2010*, 927585.
(7) Rudashevskaya, E. L.; Sacco, R.; Kratochwill, K.; Huber, M. L.; Gstaiger, M.; Superti-Furga, G.; Bennett, K. L. *Nat. Protoc.* **2013**, *8*, 75−97.
(8) Stengel, F.; Aebersold, R.; Robinson, C. V. *Mol. Cell. Proteomics* **2012**, *11*; DOI: 10.1074/mcp.R111.014027.
(9) Taatjes, D. J. *Trends Biochem. Sci.* **2010**, *35*, 315−322.
(10) Krogan, N. J.; Cagney, G.; Yu, H.; Zhong, G.; Guo, X.; Ignatchenko, A.; Li, J.; Pu, S.; Datta, N.; Tikuisis, A. P.; Punna, T.; Peregrin-Alvarez, J. M.; Shales, M.; Zhang, X.; Davey, M.; Robinson, M. D.; Paccanaro, A.; Bray, J. E.; Sheung, A.; Beattie, B.; Richards, D. P.; Canadien, V.; Lalev, A.; Mena, F.; Wong, P.; Starostine, A.; Canete, M. M.; Vlasblom, J.; Wu, S.; Orsi, C.; Collins, S. R.; Chandran, S.; Haw, R.; Rilstone, J. J.; Gandi, K.; Thompson, N. J.; Musso, G.; St Onge, P.; Ghanny, S.; Lam, M. H.; Butland, G.; Altaf-Ul, A. M.; Kanaya, S.; Shilatifard, A.; O'Shea, E.; Weissman, J. S.; Ingles, C. J.; Hughes, T. R.; Parkinson, J.; Gerstein, M.; Wodak, S. J.; Emili, A.; Greenblatt, J. F. *Nature* **2006**, *440*, 637−643.
(11) Koster, A. J.; Klumperman, J. *Nat. Rev. Mol. Cell Biol.* **2003**, *4*, SS6−SS10.
(12) Kourkoutis, L. F.; Plitzko, J. M.; Baumeister, W. *Annu. Rev. Mater. Res.* **2012**, *42*, 33−58.
(13) Kukulski, W.; Schorb, M.; Welsch, S.; Picco, A.; Kaksonen, M.; Briggs, J. A. *J. Cell Biol.* **2011**, *192*, 111−119.
(14) Baumeister, W. *Curr. Opin. Struct. Biol.* **2002**, *12*, 679−684.
(15) Vanhecke, D.; Asano, S.; Kochovski, Z.; Fernandez-Busnadiego, R.; Schrod, N.; Baumeister, W.; Lucic, V. *J. Microsc.* **2011**, *242*, 221−227.

(16) Nickell, S.; Kofler, C.; Leis, A. P.; Baumeister, W. *Nat. Rev. Mol. Cell Biol.* **2006**, *7*, 225−230.
(17) Leis, A.; Rockel, B.; Andrees, L.; Baumeister, W. *Trends Biochem. Sci.* **2009**, *34*, 60−70.
(18) Bohm, J.; Frangakis, A. S.; Hegerl, R.; Nickell, S.; Typke, D.; Baumeister, W. *Proc. Natl. Acad. Sci. U. S. A.* **2000**, *97*, 14245−14250.
(19) Beck, M.; Malmstrom, J. A.; Lange, V.; Schmidt, A.; Deutsch, E. W.; Aebersold, R. *Nat. Methods* **2009**, *6*, 817−823.
(20) Bouchet-Marquis, C.; Pagratis, M.; Kirmse, R.; Hoenger, A. *J. Struct. Biol.* **2012**, *177*, 119−127.
(21) Kemmerling, S.; Arnold, S. A.; Bircher, B. A.; Sauter, N.; Escobedo, C.; Dernick, G.; Hierlemann, A.; Stahlberg, H.; Braun, T. *J. Struct. Biol.* **2013**, *138*, 467−473.
(22) Kemmerling, S.; Ziegler, J.; Schweighauser, G.; Arnold, S. A.; Giss, D.; Muller, S. A.; Ringler, P.; Goldie, K. N.; Goedecke, N.; Hierlemann, A.; Stahlberg, H.; Engel, A.; Braun, T. *J. Struct. Biol.* **2012**, *177*, 128−134.
(23) Lim, M.; Rothschild, K. J. *Anal. Biochem.* **2008**, *383*, 103−115.
(24) Suloway, C.; Pulokas, J.; Fellmann, D.; Cheng, A.; Guerra, F.; Quispe, J.; Stagg, S.; Potter, C. S.; Carragher, B. *J. Struct. Biol.* **2005**, *151*, 41−60.
(25) Lander, G. C.; Stagg, S. M.; Voss, N. R.; Cheng, A.; Fellmann, D.; Pulokas, J.; Yoshioka, C.; Irving, C.; Mulder, A.; Lau, P. W.; Lyumkis, D.; Potter, C. S.; Carragher, B. *J. Struct. Biol.* **2009**, *166*, 95−102.
(26) Roseman, A. M. *J. Struct. Biol.* **2004**, *145*, 91−99.
(27) Tang, G.; Peng, L.; Baldwin, P. R.; Mann, D. S.; Jiang, W.; Rees, I.; Ludtke, S. J. *J. Struct. Biol.* **2007**, *157*, 38−46.
(28) Bremer, A.; Henn, C.; Engel, A.; Baumeister, W.; Aebi, U. *Ultramicroscopy* **1992**, *46*, 85−111.
(29) da Fonseca, P. C.; Morris, E. P. *J. Biol. Chem.* **2008**, *283*, 23305−23314.
(30) Martin-Benito, J.; Grantham, J.; Boskovic, J.; Brackley, K. I.; Carrascosa, J. L.; Willison, K. R.; Valpuesta, J. M. *EMBO Rep.* **2007**, *8*, 252−257.
(31) Ramadan, Q.; Gijs, M. A. *Analyst* **2011**, *136*, 1157−1166.
(32) O'Mahony, F. C.; Nanda, J.; Laird, A.; Mullen, P.; Caldwell, H.; Overton, I. M.; Eory, L.; O'Donnell, M.; Faratian, D.; Powles, T.; Harrison, D. J.; Stewart, G. D. *J. Visualized Exp.* **2013**, DOI: 10.3791/50221.
(33) Binz, H. K.; Stumpp, M. T.; Forrer, P.; Amstutz, P.; Pluckthun, A. *J. Mol. Biol.* **2003**, *332*, 489−503.
(34) Cortez-Retamozo, V.; Backmann, N.; Senter, P. D.; Wernery, U.; De Baetselier, P.; Muyldermans, S.; Revets, H. *Cancer Res.* **2004**, *64*, 2853−2857.
(35) Conrath, K. E.; Lauwereys, M.; Galleni, M.; Matagne, A.; Frere, J. M.; Kinne, J.; Wyns, L.; Muyldermans, S. *Antimicrob. Agents Chemother.* **2001**, *45*, 2807−2812.
(36) Ellington, A. D.; Szostak, J. W. *Nature* **1990**, *346*, 818−822.
(37) Li, X. M.; Mooney, P.; Zheng, S.; Booth, C. R.; Braunfeld, M. B.; Gubbens, S.; Agard, D. A.; Cheng, Y. F. *Nat. Methods* **2013**, *10*, 584.
(38) Broz, P.; Monack, D. M. *Immunol. Rev.* **2011**, *243*, 174−190.
(39) Engel, A. Assessing Biological Samples with Scanning Probes. In *Single Molecule Spectroscopy in Chemistry, Physics and Biology*; Springer: Berlin, 2010; Vol. *96*, pp 417−431.